



SHAKING-TABLE TESTS OF A FULL-SCALE FLAT-BOTTOM MANUFACTURED STEEL SILO FILLED WITH WHEAT

S. Silvestri⁽¹⁾, J. Distl⁽²⁾, M. Furinghetti⁽³⁾, I. Lanese⁽⁴⁾, S. Mansour⁽⁵⁾, M. Marra⁽⁶⁾, E. Montes⁽⁷⁾, C. Neri⁽⁸⁾, M. Palermo⁽⁹⁾, A. Pavese⁽¹⁰⁾, E. Rizzo Parisi⁽¹¹⁾, A.J. Sadowski⁽¹²⁾, F. Selva⁽¹³⁾, T. Taniguchi⁽¹⁴⁾, L. Vadrucchi⁽¹⁵⁾, F. Weber⁽¹⁶⁾

- ⁽¹⁾ Associate Professor, University of Bologna, Italy, stefano.silvestri@unibo.it
⁽²⁾ Technical Director, Maurer Engineering GmbH, Germany, J.Distl@maurer.eu
⁽³⁾ Researcher, EUCENTRE, Italy, marco.furinghetti@eucentre.it
⁽⁴⁾ Researcher, EUCENTRE, Italy, igor.lanese@eucentre.it
⁽⁵⁾ Structural Engineer, AGI FRAME Bologna, Italy, Sulyman.Mansour@framespa.it
⁽⁶⁾ Ph.D. Student, University of Bologna, Italy, matteo.marra@studio.unibo.it
⁽⁷⁾ Full Professor, University of Granada, Spain, emontes@ugr.es
⁽⁸⁾ Structural Engineer, Bologna, Italy, caterina.neri@studio.unibo.it
⁽⁹⁾ Researcher, University of Bologna, Italy, michele.palermo7@unibo.it
⁽¹⁰⁾ Associate Professor, University of Pavia and EUCENTRE, Italy, alberto.pavese@eucentre.it
⁽¹¹⁾ Research Fellow, EUCENTRE, Italy, elisa.rizzoparisi@eucentre.it
⁽¹²⁾ Senior Lecturer, Imperial College London, UK, a.sadowski@imperial.ac.uk
⁽¹³⁾ Technical Manager, AGI FRAME Bologna, Italy, Francesco.Selva@framespa.it
⁽¹⁴⁾ Professor, Tottori University, Japan, t_tomoyo@cv.tottori-u.ac.jp
⁽¹⁵⁾ Structural Engineer, AGI FRAME Bologna, Italy, Laura.Vadrucchi@framespa.it
⁽¹⁶⁾ R&D engineer, Maurer Switzerland GmbH, Switzerland, F.Weber@maurer.eu

Abstract

This paper illustrates the preliminary results of a series of shaking-table tests on a full-scale flat-bottom manufactured steel silo filled with a granular material.

The experimental campaign was developed at the EUCENTRE lab in Pavia (Italy) in February/March 2019 within the European project “SEismic Response of Actual steel SILOS (SERA-SILOS)” (<https://sera-ta.eucentre.it/index.php/sera-ta-project-18/>).

A flat-bottom cylindrical silo was tested in fixed-based and seismically isolated configurations. It is the smallest actual silo manufactured by the AGI-FRAME company (Italy). The height is $H = 5.5$ m and the radius is $R = 1.82$ m. The silo wall is realized by 5 stripes of horizontal corrugated sheets (ferrules) with thickness equal to 1 mm. The silo wall is supported by 8 vertical stiffeners characterized by an hat-shaped thin open cross-section which changes in thickness along the height. The stiffeners are connected to the silo wall by M10 7cm-spaced bolts. The silo is filled with soft wheat up to a 3.3 m height, in order to reproduce a “squat” aspect ratio $H/2R$ roughly equal to 1. The weight of the steel silo itself is around 12 kN, the amount of grain is around 285 kN, the 4.8m \times 4.8m \times 0.4m r.c. plate is 230 kN weigh. The isolators placed between the table and the r.c. plate are Curved Surface Sliders friction pendulum devices expressly manufactured by the MAURER company (Germany – Switzerland) to obtain a 3 s period of vibration (radius = 2.2364 m, max allowable displacement = 20 cm).

Mono-axial shaking-table tests were performed using random signals, low-frequency sinusoidal inputs and earthquake records (both artificial and real). The following sensors were utilized: uniaxial and triaxial accelerometers placed at different heights of the silo, vertical strain gauges on the external surfaces of the stiffeners, four load cells placed at two heights of the silo, LVDTs between the isolated system and the table, and HD video-cameras to monitor the spatial displacements of the main structural elements.

The main objectives of the shaking-table tests were: (i) to identify the basic dynamic properties (period of vibration, damping ratio, amplification) of the grain-silo system, (ii) to experimentally assess the static pressure during the filling phase and the dynamic over-pressures during the shaking-table tests, and (iii) to evaluate the benefits obtained introducing an isolation system at the base of the silo.

Keywords: steel silo, shaking-table tests, dynamic properties, pressures, seismic isolators



1. Introduction

The structural design of steel flat-bottom ground-supported silos containing granular material represents a challenging issue. They differ from many other civil structures since the weight of the silo structure is sensibly lower than the one of the ensiled particulate material and, in case of earthquake ground motion, the particle-structure interaction plays a fundamental role on the global dynamic response. The complex mechanism through which the ensiled material interacts with the silo wall has been studied since the XIX century [1][2][3][4][5]. Nonetheless, several issues are still to be addressed regarding “grain-silo systems” and structural failures still occur [6].

This paper presents the preliminary results of a shaking-table experimental campaign developed at the EUCENTRE lab in Pavia (Italy) in February/March 2019 within the European project “SEismic Response of Actual steel SILOS (SERA-SILOS)” (<https://sera-ta.eucentre.it/index.php/sera-ta-project-18/>). The main objectives of the shaking-table tests were: (i) the identification of the basic dynamic properties (frequency, damping ratio, amplification) of the grain-silo system, (ii) the experimental assessment of the static pressure (during filling phase) [7] and seismic dynamic over-pressures exerted by the ensiled material on the silo wall [8][9][10][11][12], and (iii) the assessment of the benefits obtained introducing a isolation system at the base of the silo.



Fig. 1 – The tested silo and constructive details.



2. The tested silo and the ensiled content

A flat-bottom cylindrical silo has been tested on fixed restraints and on seismic isolators (fixed-base and isolated-base configurations, respectively). It is the smallest actual silo manufactured by the Italian company AGI-FRAME (Fig.1).

The total height including the inclined roof is $H = 5.5$ m and the radius is $R = 1.82$ m. The silo wall is realized by 5 stripes of horizontal corrugated sheets (ferrules) with thickness equal to 1 mm. Each strip is high 881 mm. The silo wall is supported by 8 vertical stiffeners characterised by a hat-shaped thin open cross-section which changes in thickness along the height (from the top to the bottom: 1.5, 2, and 3 mm). Ferrules and stiffeners are made of S350GD steel with Z450 galvanization. The stiffeners are connected to the silo wall by M10 (class 8.8, hot galvanized) 0.07 m-spaced bolts. The silo roof is made by 16 inclined metal sheets.

The silo is filled in quasi-concentric way up to 3.3m height with soft wheat, in order to achieve an aspect ratio $H/2R$ roughly equal to 1 which corresponds to the upper limit of the squat silo category according to EN1991-4:201116. Specific weight of the used wheat is 8.04 kN/m³; grain-grain friction coefficient and pressure ratio are tentatively estimated to be around 0.55 and 0.60, respectively, but specific tests are currently under development. The average diameter of the particles is 2.5 - 3mm, with no more than 4% of fine material of diameter less than 2mm based on the result of particle size distribution test and manual measurements. The tests were performed in a closed laboratory environment where the temperature was 16° C and the humidity was in the range 30%-45%.

The isolators put between the table and the r.c. plate are Curved Surface Sliders friction pendulum devices expressly manufactured by the MAURER company (Germany – Switzerland) in order to obtain a 3 s period of vibration (radius = 2.2364 m, max allowable displacement = 0.2 m).

The weight of the steel silo itself is around 12 kN, the amount of grain is around 285 kN, the weight of the 4.8 m \times 4.8 m \times 0.4 m r.c. plate is 230 kN.

3. Testing instrumentation

The following sensors have been utilized: vertical strain gauges on the external surfaces of the stiffeners (at $z = 42$ cm from the r.c. plate, Fig. 2a), uniaxial and triaxial accelerometers placed at different heights of the silo (Fig. 2b), four load cells (Fig. 2c) placed on the internal side of the wall at two heights of the silo in order to measure the horizontal pressure between the grain and the wall, and an optical system (HD video-cameras + markers) to monitor the displacements of stiffeners, silo wall, roof, r.c. plate and shaking-table. Load cells and strain gauges have been activated also in the filling phase (realised in 3 different sessions: 150 kN, 100 kN and 35 kN amount of grain, for a total time of 3 hours), as well as in the discharging phase.

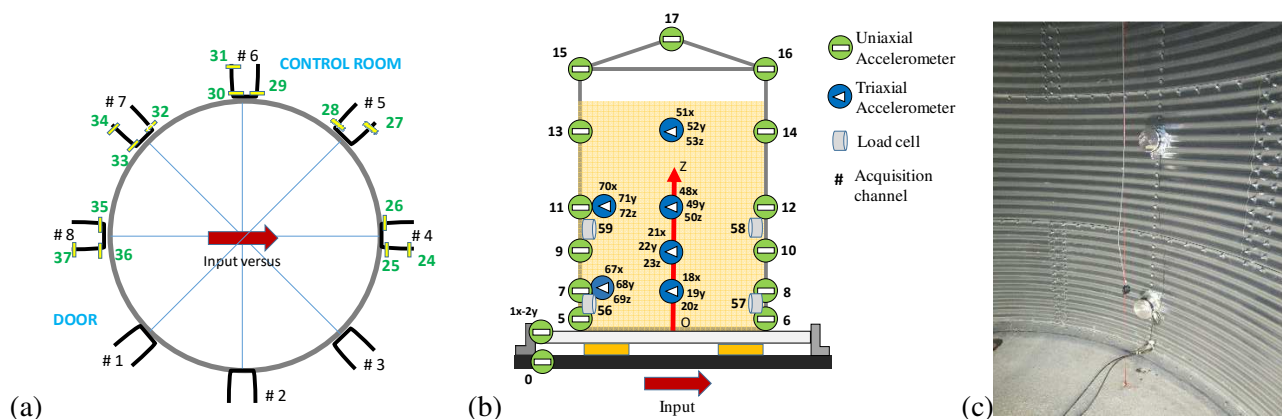


Fig. 2 – (a) Vertical strain gauges on the stiffeners. (b) Accelerometers. (c) Load cells



4. Testing program

Mono-axial shaking-table tests have been performed using random signals, low-frequency sinusoidal inputs (to roughly reproduce the ideal conditions of "constant acceleration", i.e. to achieve a large duration for which the acceleration can be reasonably considered constant in time around the peak of the sinusoid) and three earthquake records: rs1 earthquake (real record of the Campano Lucano Italy 23/11/1980 earthquake, identified as a "far-from-resonance frequency content" input), a1 artificial earthquake, rs3 earthquake (real record of the Kalamata Greece 13/09/1986 earthquake, identified as a "close-to-resonance frequency content" input, namely a demanding one for the grain-silo system). Table 1 provides the sequence of the performed tests.

Table 1 – List of the performed shaking table tests

FIXED-BASE			ISOLATED-BASE		
Peak Table Acceleration	Test Number	Type of signal	Peak Table Acceleration	Test Number	Type of signal
0.07 g	1	random	0.05 g	148-165	random
0.10 g	2-9	sin 0.5 Hz	0.10 g	166-168	a1 eqke
	10-13	rs1 eqke	0.30 g	169-170	random
	14-16	a1 eqke	0.10 g	171-174	a1 eqke
	17-19	rs3 eqke	0.20 g	175-179	a1 eqke
0.15 g	20-21	random	0.15 g	180-182	random
0.20 g	22-26	sin 1 Hz	0.30 g	183-187	a1 eqke
	29-31	rs1 eqke	0.20 g	188	random
	32-34	a1 eqke	0.40 g	189-193	a1 eqke
	35-38	rs3 eqke	0.45 g	194	a1 eqke
	39-40	random	0.50 g	195	a1 eqke
0.30 g	41-45	sin 1 Hz	0.55 g	196	a1 eqke
	46-48	rs1 eqke	0.20 g	198-200	random
	49-51	a1 eqke	0.10 g	201-205	rs3 eqke
	53-55	rs3 eqke	0.20 g	206-210	rs3 eqke
0.40 g	56-59	sin 1 Hz	0.30 g	211-215	rs3 eqke
	60-62	rs1 eqke	0.40 g	216-220	rs3 eqke
	63-66	a1 eqke	0.45 g	221	rs3 eqke
	67-69	rs3 eqke	0.50 g	222	rs3 eqke
0.50 g	71-76	sin 1 Hz	0.55 g	223	rs3 eqke
	77-80	rs1 eqke	0.10 g	224-227	rs1 eqke
	81-83	a1 eqke	0.20 g	228-232	rs1 eqke
	84-86	rs3 eqke	0.25 g	233	rs1 eqke
	88-89	random	0.30 g	234-235	rs1 eqke
0.07 g	88-89	random	0.35 g	236	rs1 eqke
0.15 g	90-91	random	0.10 g	238-242	pulse
0.20 g	92-93	random	0.20 g	243-247	pulse
0.25 g	94-96	random	0.30 g	248	pulse
0.10 g	97-101	sin 0.5 Hz	0.10 g	249-253	sin 0.7 Hz
0.20 g	102-106	sin 1 Hz		254-256	sin 0.6 Hz
0.30 g	107-111	sin 1 Hz			
0.40 g	112-116	sin 1 Hz			
0.50 g	117-121	sin 1 Hz			
0.60 g	122	rs3 eqke			
	123	rs1 eqke			
	124	rs3 eqke			
	125	a1 eqke			
0.10 g	126-129	sin 5 Hz			
	130-134	sin 6 Hz			
	135-139	sin 7 Hz			
	140-145	sin 8 Hz			



5. Test results

5.1 Filling phase

During the filling of grain into the silo, data have been recorded. Hereafter illustrative plots are reported which show the pressure values captured by the four load cells (Fig. 3a) and the strain values measured in three different points of the cross section at the base (42 cm from the r.c. plate) of stiffener # 4 (Fig. 3b).

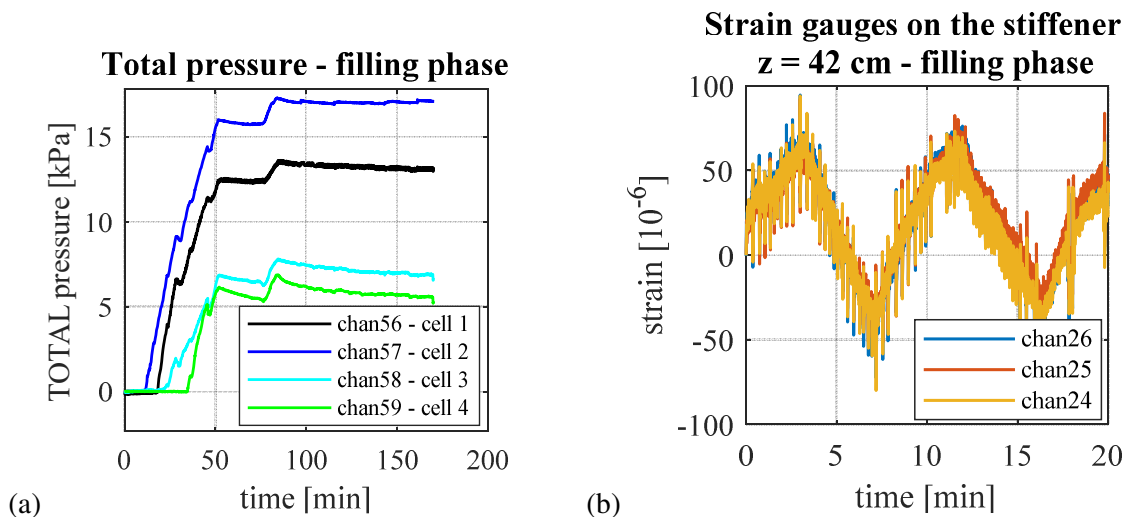


Fig. 3 – (a) Horizontal pressure during filling. (b) Strain values window at the base of stiffener n. 4 during filling phase

It can be noticed that the grain has been introduced from the top opening of the roof with a small eccentricity leading to a cell (n. 2) loading first than the one on the other side (n. 1). Also, from a qualitative point of view, the plot is consistent with the Janssen (1895) [1][2][7] static pressure model. The strain plots highlight a strange periodic (period about 8 min) behaviour of the stresses in the stiffeners. It seems to be ascribed to a physical phenomenon that should still be interpreted (maybe related to the corrugation waves of the silo wall).

5.2 First session of tests: fixed-base configuration

The experimental frequencies have been obtained from the response of the silo as subjected to white-noise random signals for various peak table acceleration levels. The system transfer function has been obtained as the square root of the ratio of the periodogram (which is an estimate of the Power Spectral Density, using Welch method with Hamming windows [13]) of the acceleration signal registered at a given level divided by the periodogram of the table acceleration signal.

Table 2 collects the frequencies as evaluated both before and after grain compaction. Compaction appeared for table accelerations larger than 0.5 g (tests n. 71-83), almost consistent with the value of the grain-grain friction coefficient (around 0.55): the grain free-surface has been kept monitored during the tests by visual method and four vertical graduated bars. It can be noticed that the fundamental frequency of the grain-silo system depends on both the acceleration and the compaction level: it decreases with increasing acceleration (more “effective mass” [8][9][10][11][12]) and it increases with increasing compaction (higher stiffness provided by grain material).

Illustrative plots of the estimate of the Power Spectrum Density of the input signal (accelerometer n. 1 on the r.c. plate) and of the output signal (accelerometer n. 13 on the stiffener at height 2.85 m) are reported in Fig. 4a, as obtained for the 0.15g random input test (tests n. 90-91). Fig. 4b compares the square root of their ratio, i.e. the module of the transfer function of the grain-silo system (red colour), with a first rough approximation of the module of the transfer function, as obtained by simply dividing the FFTs of the two signals (black colour).



Table 2 – Experimental frequencies

Peak Table Acceleration	First set of tests before grain compaction		Second set of tests after grain compaction	
	Test N.	f (Hz)	Test N.	f (Hz)
RND				
0.07 g	1	10.8	88; 89	12.3
0.15 g	20; 21	10.0	90; 91	11.3
0.20 g	39; 40	10.3	92; 93	10.7
0.25 g	-	-	94; 95; 96	10.7

Similarly, it is possible to obtain the transfer functions of the system considering earthquake signals at different acceleration levels (Fig. 5a and b). The figures show that the dynamic amplification increases along the height of the silo and decreases with the input acceleration level, due to a simultaneous increase in the damping ratio. From the transfer function amplitude of the grain-silo system, a rough indication on the damping ratio can be inferred: if a maximum amplification around 3 is considered for the resonance frequency, then a damping ratio around 18% is obtained. This is also observed applying the half-power bandwidth method (SDOF assumption) to the transfer functions.

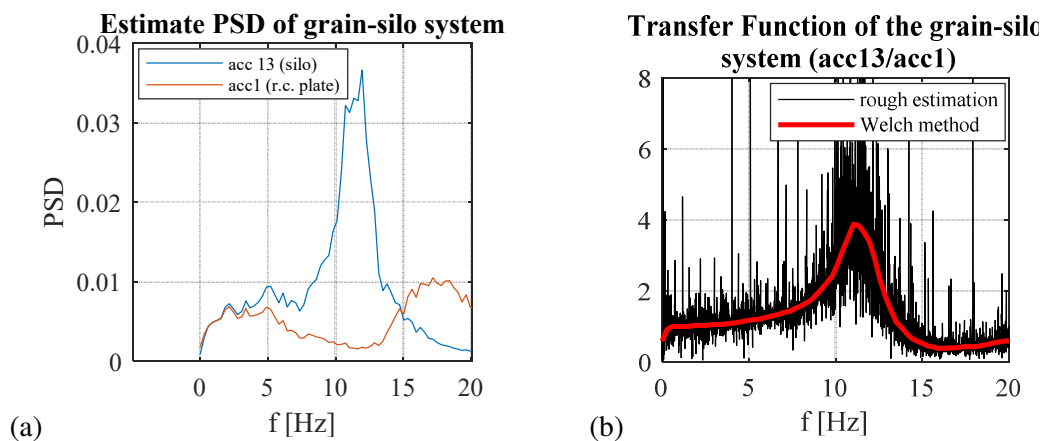


Fig. 4 – (a) PSD estimate. (b) Transfer function of the grain-silo system

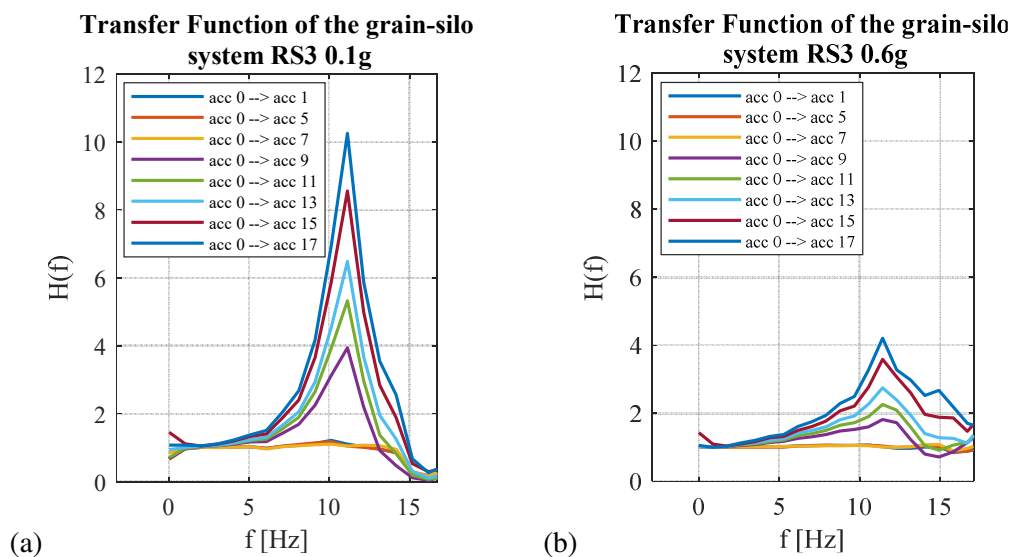


Fig. 5 – Transfer functions of the grain-silo system, as obtained for: (a) rs3 0.1g, (b) rs3 0.6g



As far as the dynamic amplification of the grain-silo system is concerned, Fig. 6 displays the so-called Peak Acceleration Profiles, as they collect the maximum accelerations measured at different heights of the silo wall, for two types of signal: 1 Hz sinusoidal and rs3 earthquake for several tests with different Peak Table Accelerations. It can be noticed that the response of the grain-silo system is substantially not affected by dynamic amplification for the sinusoidal input (Fig. 6a), whilst a slight amplification (1.3-1.5 at the level of grain, and 1.4-1.8 at the base roof level) is observed for the rs3 earthquake (Fig. 6b) which is a “close-to-resonance frequency content” real record. Again, the dynamic amplification seems to decrease for increasing Peak Table Acceleration from 0.1 g to 0.4 g. This may be ascribed to a higher damping ratio provided by the grain.

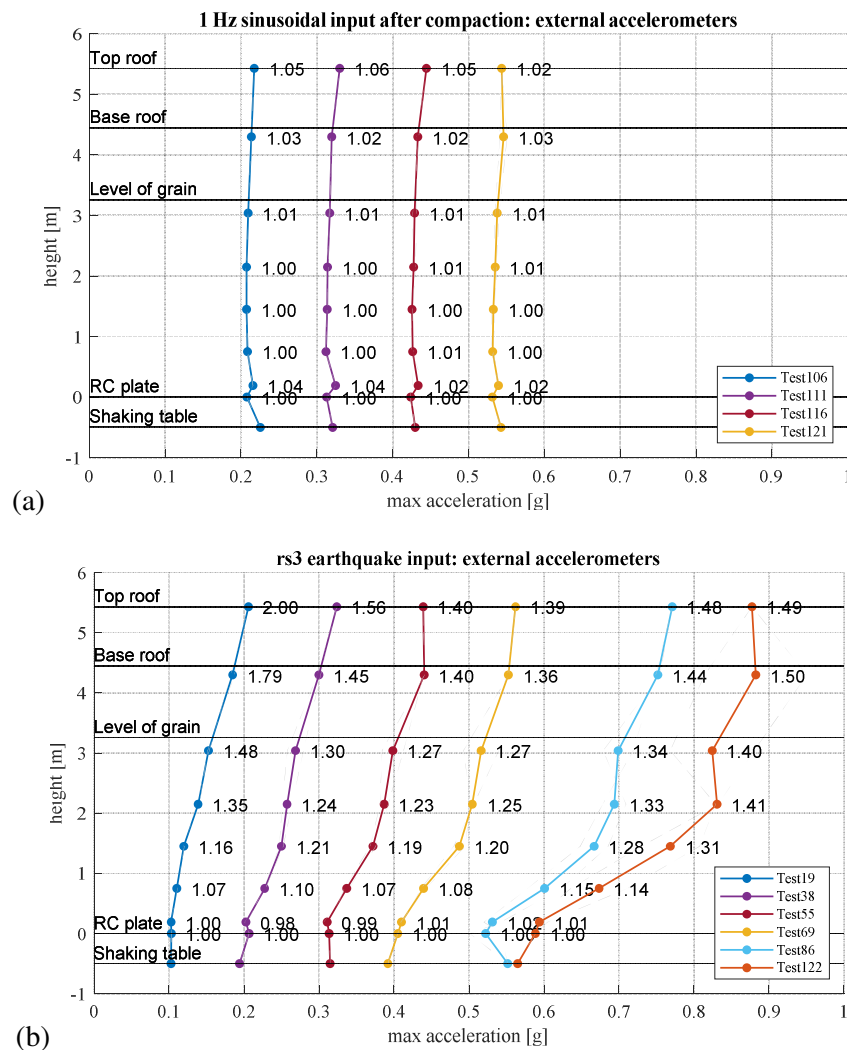


Fig. 6 – Peak Acceleration Profiles and dynamic amplification factors for (a) 1 Hz sinusoidal input and (b) rs3 earthquake input

As far as the pressures exerted by the grain on the silo wall are concerned, the following Fig. 7a and b report the values measured by the specially designed pressure cells placed at two heights of the silo wall, for the 0.3 g 1 Hz sinusoidal input and for the 0.3 g rs3 earthquake input, respectively.

Fig. 8a and b compare the dynamic overpressures measured at different acceleration levels for the 1 Hz sinusoidal and the rs3 earthquake inputs. It can be noticed that the measured dynamic pressure values increase from the top to the bottom of the silo, somehow following a linear profile.



Fig. 9a shows the dependence of the dynamic overpressure profile on the nominal Peak Table Acceleration for the a1 artificial earthquake input. It can be noticed that the dynamic pressure increases almost linearly with the acceleration level.

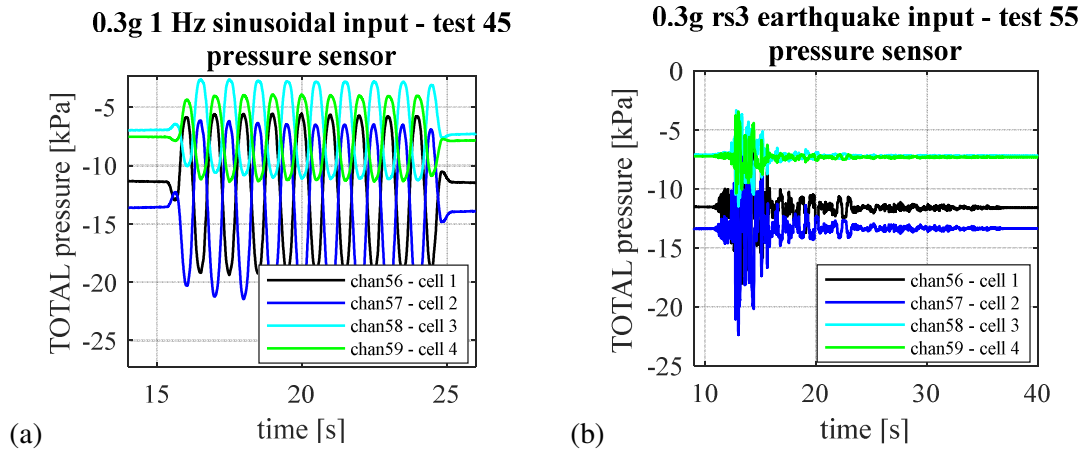


Fig. 7 – Horizontal pressures measured by the four load cells during two tests

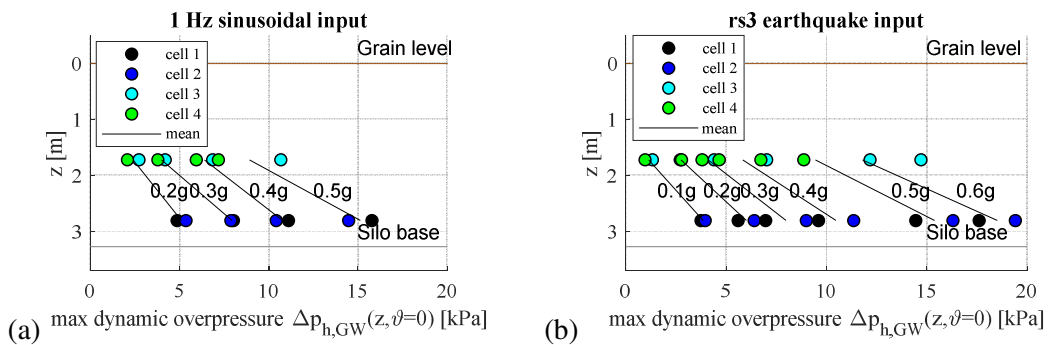


Fig. 8 – Maximum horizontal pressures measured by the four load cells for various (a) sinusoidal and (b) earthquake tests

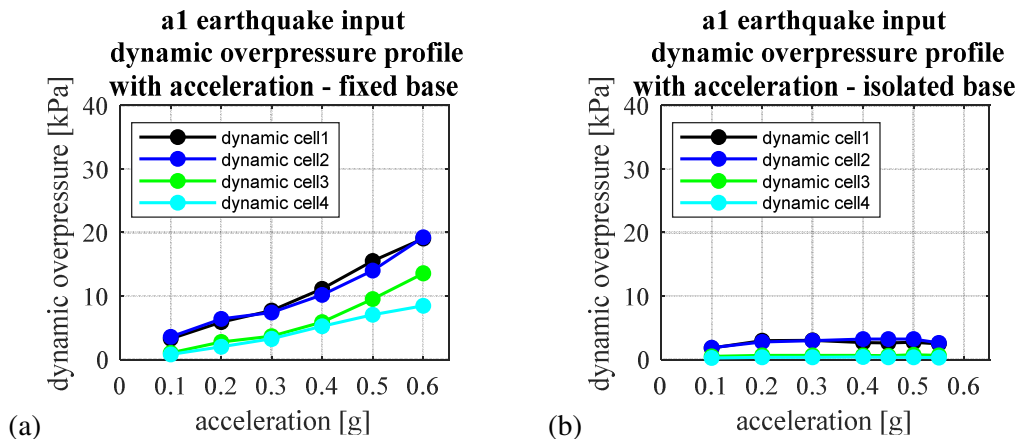


Fig. 9 – Dynamic overpressure profile with nominal Peak Table Acceleration for a1 earthquake input for (a) fixed-base and (b) isolated-base



Fig. 10 displays the displacement profile, measured with HD video-cameras, at the time instant at which the maximum displacement of the marker at the top of Stiffener #8 is captured with the corresponding displacement of the other markers on the stiffeners on the same radial (#4 and #8). The maximum relative displacement (with respect to the r.c. plate) reached at the highest monitored point at Stiffener #8 is 3.3 mm, whilst for the corresponding point close to the grain surface level is 2.15 mm.

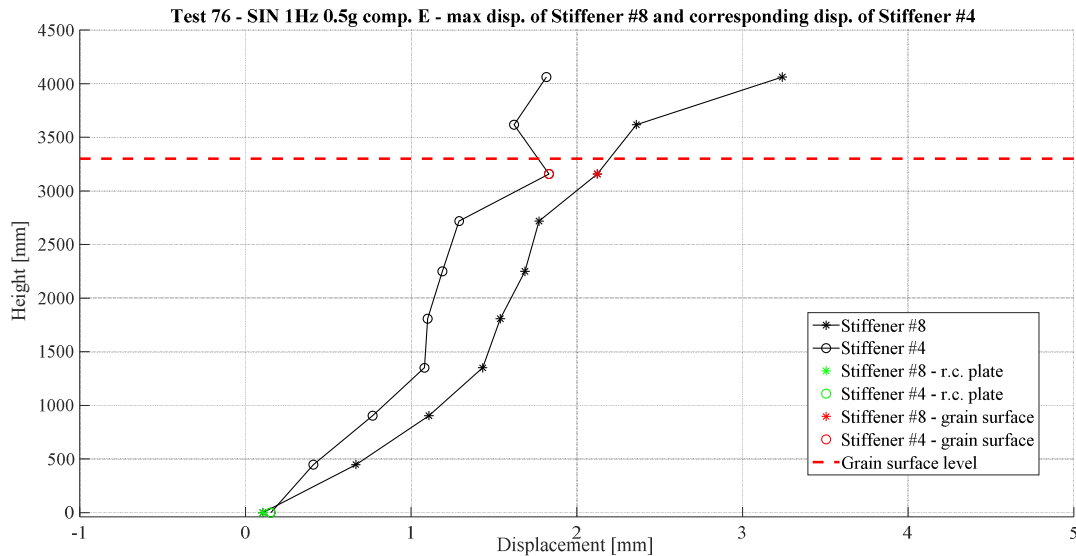


Fig. 10 – Displacement profile of stiffeners #4 and #8 at the time instant corresponding to the maximum displacement of the highest point of Stiffener #8 during test n.76

5.3 Second session of tests: isolated-base configuration

The silo has also been tested in seismically isolated conditions, by removing the steel anchorages used to fix the r.c. plate to the table in the first fixed-base configuration.

Fig. 9b shows the dependence of the dynamic overpressure profile on the nominal Peak Table Acceleration for the a1 artificial earthquake input. It can be noticed that the pressure, for inertia forces larger than the friction forces of the Curved Surface Sliders pendulum devices (namely, for accelerations larger than 0.05 g - 0.10 g), is constant and independent of the Peak Table Acceleration. The comparison between Fig. 9a and b highlights the effectiveness of base isolation in breaking down the dynamic overpressure on the silo wall.

Fig. 11a and b display the relative displacement between the table and the superstructure (silo on the r.c. plate), i.e. the displacement developed by the isolators, for the rs1 and rs3 earthquake inputs, both scaled at 0.3 g. Two simple 2-dofs models have been prepared to predict this maximum relative displacement: one linear equivalent model with friction coefficient equal to 5%, and another non-linear model with friction coefficient equal to 8%. It can be noticed that the non-linear model is capable of well capturing the measured displacement.

Fig. 12 displays the Peak Acceleration Profiles for the a1 earthquake input: the acceleration that reaches the base of the silo is, in all cases, around 0.1 g, comparable with the friction coefficient of the isolators.

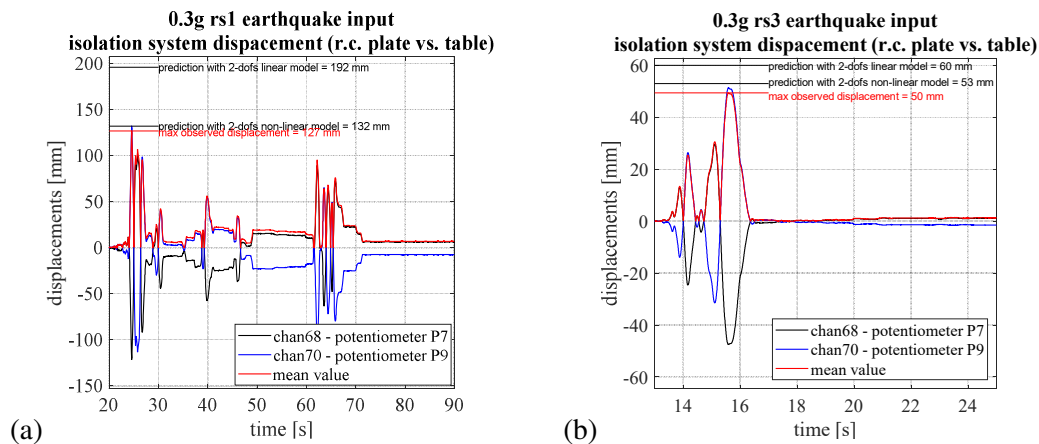


Fig. 11 – Relative displacements developed by the isolators placed between the table and the superstructure (silos on the r.c. plate) for the rs1 (a) and rs3 (b) earthquake inputs, both scaled at 0.3g

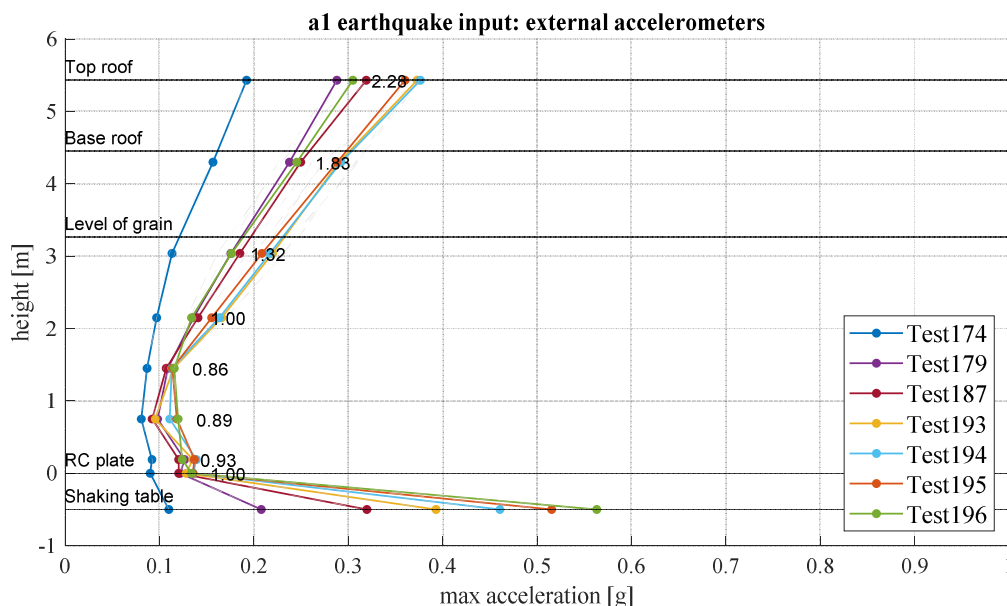


Fig. 12 – Peak Acceleration Profiles and dynamic amplification factors for a1 earthquake input

6. Static pressure values during the experimental campaign

During the whole experimental campaign (from the filling day, 20-Feb-2019, up to the final day of the tests, 5-Mar-2019), it was possible to record the static pressures produced by the grain on the silo wall in four points. Fig. 13 displays the static pressure values as captured by the four load cells before each single test. Cells 1 and 2 were placed at 0.42 m from the r.c. plate, while cells 3 and 4 at 1.50 m.

Many interesting issues have been noticed and are still under study. The initial pressures at the end of the filling day are not symmetrical (cell 2 provides a larger value than cell 1, and the same for cell 3 with respect to cell 4) as expected, due to non-concentric filling. The dynamic tests started after five days, during which cell 2 recorded an increase in the pressure, cell 3 a decrease, whilst cell 1 and 4 (on the other side) showed no changes. During the first dynamic tests, cells 1 and 2 at the lower level tended to reach similar values, close to the linear (geostatic) pressure model prediction. The same occurred for cells 3 and 4 at the higher level. Generally speaking, dramatic changes in the pressure values have been observed (e.g. high-



intensity random vibration may switch the maximum pressure from one side to the other side of the silo). Moreover, an unexpected significant drop in the pressure values occurred during the repose day (28-Feb-2019) between the fixed-based (FIX) and isolated-based (ISO) configurations. Some similar but smaller changes can be noticed during the nights between the testing days (small drops during FIX tests and small increases during ISO tests). Finally, during the ISO tests, no big changes happened, maybe due to the protection offered by the seismic isolators. In this phase, the static values of the pressures are close to the Janssen pressure model.

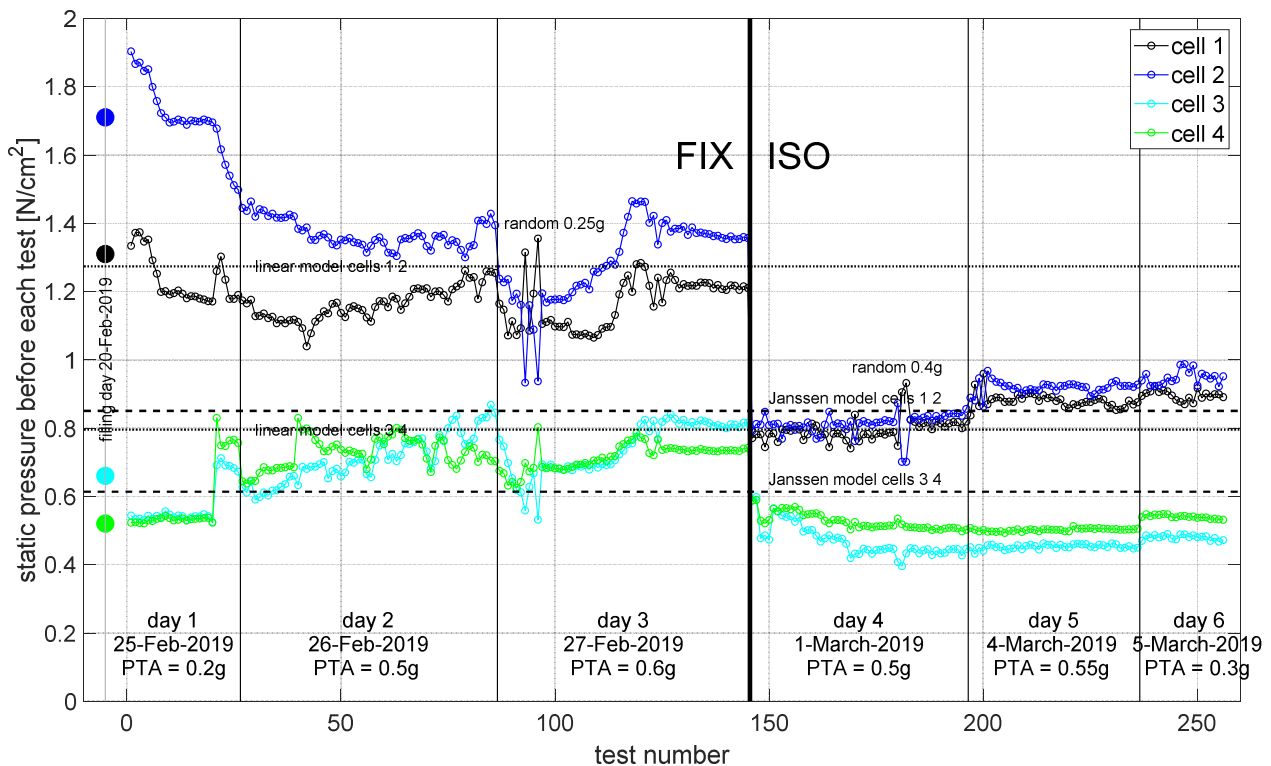


Fig. 13 – Static pressure values as recorded by the four load cells before each single test

7. Conclusion

This paper reports on the filling phase recording and a number of shaking-table tests on a 5.5m-high 3.64m-diameter actual flat-bottom cylindrical steel silo in fixed-base and isolated-base conditions. The silo is filled in quasi-concentric way up to 3.3m height with soft wheat, in order to achieve an aspect ratio $H/2R$ roughly equal to 1. A general overview and preliminary results are presented. The horizontal pressure distribution during the filling phase is qualitatively consistent with the Janssen static pressure model, but quantitatively closer to the linear geostatic one. As far as the dynamic results are concerned, the resonance frequency is around 11 Hz and slightly changes according to acceleration intensity, type of signal and grain compaction level. The dynamic amplification increases along the silo height and decreases with the acceleration, according to an increase in the damping ratio. The measured dynamic pressure values seem to have a linear trend with the silo height. The isolation system is effective in reducing the dynamic pressures and the accelerations on the silo superstructure.



8. Acknowledgements

This project “SEismic Response of Actual steel SILOS (SERA-SILOS)” (<https://sera-ta.eucentre.it/index.php/sera-ta-project-18/>) has received funding from the European Union’s Horizon 2020 research and innovation programme under grant agreement No 730900.

9. References

- [1] Janssen H (1895): Versuche uber Getreidedruck in Silozellen. *Z. Ver. Dtsch. Ing.*, **39** (35), 1045-1049.
- [2] Koenen M (1896): Berechnung des Seiten und Bodendrucks in Silozellen. *Centralblatt der Bauverwaltung*, **16**, 446-449.
- [3] Reimbert ML, Reimbert AM (1976): *Silos: Theory and Practice*. Trans Tech Publications: Clausthal, Germany, 1st edition
- [4] Rotter J, Hull T (1989): Wall loads in squat steel silos during earthquakes. *Engineering Structures*, **11** (3), 139-147.
- [5] Rotter J (2001): *Guide for the economic design of circular metal silos*. CRC Press, 1st edition.
- [6] Dogangun A, Karaca Z, Durmus A, Sezen H (2009): Cause of damage and failures in silo structures. *Journal of performance of constructed facilities*, **23** (2), 65-71.
- [7] EN 1991-4: 2006 Eurocode 1 - Actions on structures - Part 4: Silos and tanks.
- [8] EN 1998-4: 2006 Eurocode 8: Design of structures for earthquake resistance - Part 4: Silos, tanks and pipelines.
- [9] Holler S, Meskouris K (2006): Granular material silos under dynamic excitation: numerical simulation and experimental validation. *Journal of Structural Engineering*, **132** (10), 1573-1579.
- [10] Silvestri S, Gasparini G, Trombetti T, Foti D (2012): On the evaluation of the horizontal forces produced by grain-like material inside silos during earthquakes. *Bulletin of Earthquake Engineering*, **10** (5), 1535-1560.
- [11] Pieraccini L, Silvestri S, Trombetti T (2015): Refinements to the Silvestri’s theory for the evaluation of the seismic actions in flat-bottom silos containing grain-like material. *Bulletin of Earthquake Engineering*, **13** (11), 3493-3525.
- [12] Silvestri S, Ivorra S, Di Chiacchio L, Trombetti T, Foti D, Gasparini G, Pieraccini L, Dietz M, Taylor C (2016): Shaking-table tests of flat-bottom circular silos containing grain-like material. *Earthquake Engineering & Structural Dynamics*, **45**, 69-89.
- [13] Allen RL, Mills D (2004): *Signal analysis: time, frequency, scale, and structure*. John Wiley & Sons, 1st edition.